AD-A071 028 VIRGINIA POLYTECHNIC INST AND STATE UNIV BLACKSBURG --ETC F/G 20/4
LIQUID FUEL JET INJECTION INTO A SIMULATED SUBSONIC 'DUMP' COMB--ETC(U)
MAY 79 J C OGG, J A SCHETZ AFOSR-78-3485

UNCLASSIFIED VPI-AERO-093 AFOSR-TR-79-0769 NL

/ OF |
AD
A071 028

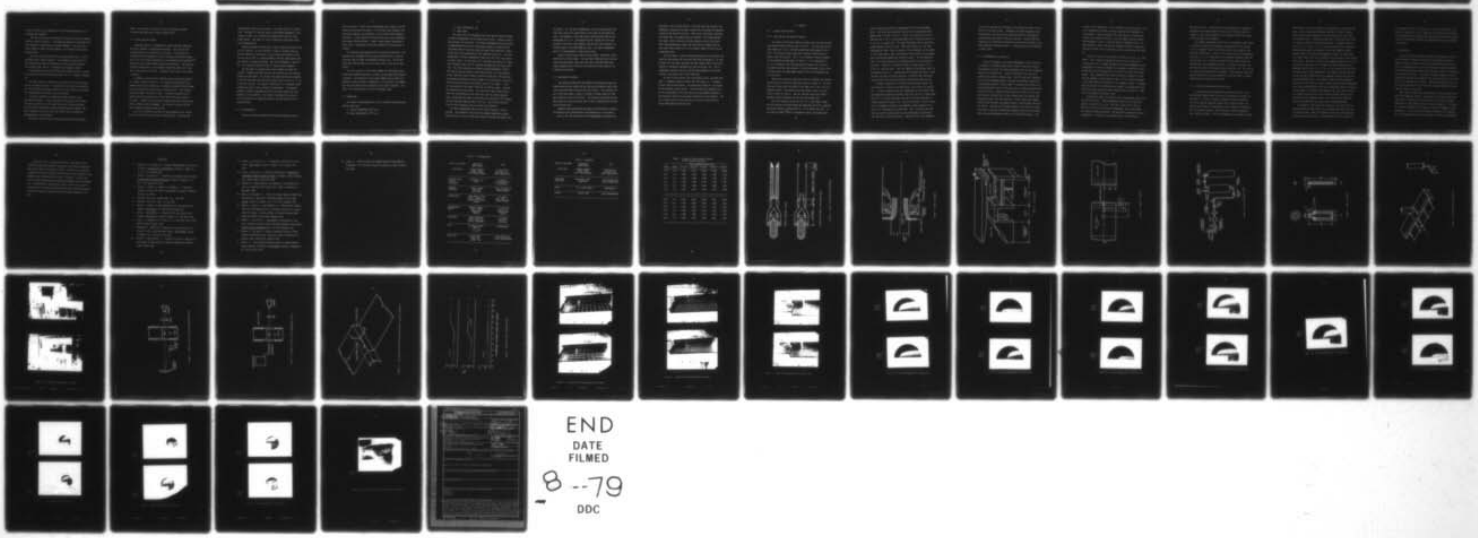

END
DATE
FILMED
8 --79
DDC

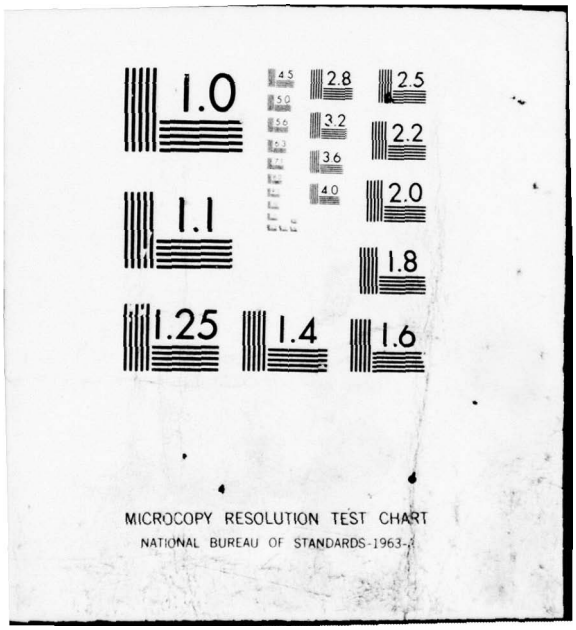
1.0
1.1
1.25
1.4
1.6
1.8
2.0
2.2
2.5
2.8
3.2
3.6
4.0
4.5
5.0
5.6
MICROCOPY RESOLUTION TEST CHART
NATIONAL BUREAU OF STANDARDS-1963-A

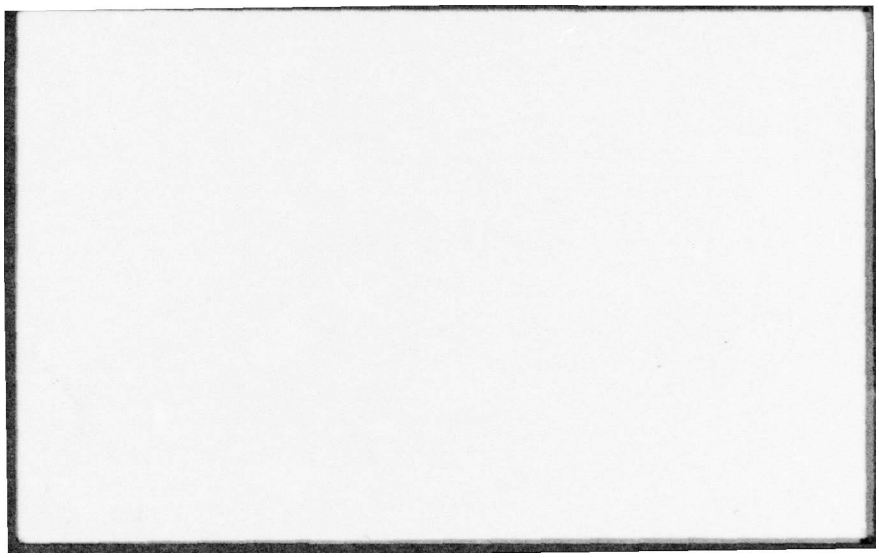

AFOSR-TR
May 1979

VPI-Aero-093

See 1473 in back.

LIQUID FUEL JET INJECTION INTO A SIMULATED SUBSONIC "DUMP" COMBUSTOR

John C. Ogg and Joseph A. Schetz

Aerospace and Ocean Engineering Department

TABLE OF CONTENTS

NOMENCLATURE

d	Distance from injection port to step
h	Step height
P	Static pressure
P_o	Total pressure
$P_{o,\infty}$	Total pressure in plenum chamber of wind tunnel
$\bar{q}$	Ratio of the dynamic pressure of the jet to the dynamic pressure of the freestream
V_j	Mean velocity of the injectant
X	Streamwise coordinate of test model
Y	Vertical coordinate of test model
Z	Transverse coordinate of test model
ρ_j	Density of injectant

1.0 INTRODUCTION

1.1 Background

Until very recently, the ramjet engine had fallen into disuse as a propulsion system for missiles. Today, however, because of its low altitude, high-speed performance and efficiency, development and use of the ramjet is being continued. The concept of one type of ramjet, the integral rocket/ramjet (IRR), was originally developed by the Navy in the early 1950's. Later, in 1973 tests were conducted in conjunction with the Navy's Air Launched Low Volume Ramjet (ALVRI) program, confirming the potential of the IRR for improving propulsion performance and lowering the cost of tactical missiles.[1] Today the Air Force is concentrating on developing the integral rocket/ramjet for its advanced strategic air-launched missile (ASALM).[2] This type of propulsion system was chosen because launching of missiles from aircraft places severe constraints on missile volume, and the integral rocket/ramjet is smaller than conventional ramjet configurations.

Ramjets require high velocities to sustain combustion, and the high initial velocity is usually attained with a rocket booster phase. The advantage of the integral rocket/ramjet concept over conventional ramjets is that the booster rocket is contained within the ramjet engine instead of being externally mounted on the missile. The integral rocket/ramjet utilizes the combustion chamber as the casing for the boost grain, thereby reducing the size of the total rocket/ramjet propulsion system. As seen in Figure 1, in the initial booster phase of flight, the combustion chamber serves as a rocket engine. After the

boost grain is expended, the port cover at the forward end of the combustion chamber is blown inward. Also the nozzle inserts (shown in black) are jettisoned, and propulsion is then sustained by liquid fueled ramjet operation. But, because the ramjet engine must house the rocket, the combustion chamber cannot be designed for optimal ramjet operation. As shown in Figures 1 and 2, the conventional flame holding devices are replaced by sudden expansion geometry, and liquid fuel is injected in the inlet region of the engine upstream of the step. The combustion process is dependent on the penetration, break-up and mixing of the liquid fuel with the inlet air, where penetration is the transverse distance the liquid jet travels into the flowfield. Efficiency of the combustion process is a determining factor in the overall size and weight of the missile.

Liquid jet injection into subsonic and supersonic flowfields has been extensively investigated in order to predict the behavior of liquid jets injected into airstreams. Cross-flow injection has applications other than combustion of liquid fuel in ramjets and dump combustors. These include vehicle side force attitude control, transpiration cooling and thrust vector control. An investigation was done by Schetz et.al.,[3] of injection through a flat plate model into high subsonic speed air streams to determine jet penetration and breakup. Those results are directly applicable to the IRR flowfield. Also included in the report was a comprehensive review of prior available literature in this field. In the investigation, the functional dependence of penetration, injector geometry and flowfield parameters for

high speed subsonic flowfields was analytically and experimentally investigated. A correlation equation for penetration was developed.

Studies of break-up of a liquid jet go back very far with the first meaningful analysis presented by Lord Rayleigh[4,5] for the case of a liquid jet entering a medium of quiescent gas. But it was not until 1961 that Mayer[6] developed an analysis of a liquid jet in a gas crossflow. Previous to this, owing to the complexity of the physical phenomena involved in the process, the study of liquid atomization in the high velocity gas flow was pursued principally by empirical methods. Since then much work, both analytical and experimental, has been done on jet penetration breakup and atomization. See references (7 - 14). In one of the most recent investigations (Nejad, et. al.),[15] it was determined that the mean diameter of droplets resulting from crossflow breakup and atomization could be accurately determined using a diffractively scattered light technique (Mia scattering).

Another aspect of dump combustor flowfields is the sudden expansion geometry. Sudden expansion flowfields commonly occur in many engineering applications; sudden enlargements in piping, orfice plates used for flow measurement and combustion in fireboxes such as used in steam generators. Abbot & Kline[16] defined three distinct regions in the quasi-steady viscous stall region behind a two dimensional rearward facing step: a three dimensional zone of separation (imbedded vortices) immediately downstream of the step, a two dimensional recirculation zone and a time dependent tail region. They found for area

expansion ratios of less than 1.5,that a symmetrical arrangement of two rearward facing steps yielded stall regions equal in length to that of a single step of the same area expansion ratio. They also concluded that the flow pattern was essentially independent of inlet boundary layer configuration. Interpreting their data, it appeared that reattachment occured about 6 step heights down stream of the step for area expansion ratios of less than 1.5. Two dimensional investigation allows an excellent view of the flowfield, but most engineering applications are of annular or axisymmetric geometries. Recently Kangovi and Page[17] investigated this situation for turbulent flow using hot wire anemometers and pressure surveys. They found a 2 - 3% influence on inlet Mach number upstream of the step depending on step height and incoming Mach number. They concluded that the reattachment point was 8 step heights downstream of the step for area ratios less than 1.6. Drewry[18,19] found reattachment between 8 - 9 step heights downstream of the step for area expansion ratios of 2.4. In both of the preceding cases, it was found that full pressure recovery occurred well downstream of the reattachment.

The purpose of the present investigation was to study the fuel/injectant interaction in a "dump" combustor as a function of step height, injection port location and the ratio of the dynamic pressure of the injectant to the dynamic pressure of the air and hence the injectant flow rate. The investigation was done in two dimensional, cold flow to permit study of the details of the fluid mechanics.

1.2 Scope of Investigation

This work concentrated in three areas pertinent to fuel injection into dump combustors, such as those found in integral rocket-ramjets. The first objective of this work was to design and build a high speed, subsonic, sudden-expansion test section to simulate a dump combustor. The test section was to be used in the 9 x 9 in. supersonic/transonic wind tunnel at VPI&SU. To be included in the design was the capacity to inject liquids normal to the flow at various locations upstream of the step into the combustor.

The second objective was to extend the work of Schetz, et.al.[3] on penetration and break-up of a transversely injected liquid jet into high subsonic speed air streams. Their work in this area "was to study the effect of:

1) Shape of the injector
2) Size of the injector, and
3) Orientation of the injector with respect to the air stream

on the observable characteristics of the jet:

1) Penetration,
2) Structure of the jet column,
3) Droplet size distribution, and
4) Possible existence of liquid surface layer"[3]

Thus, a primary objective of the present work was to correlate the effect of geometry of the combustor (particularly the step height and injector location relative to the step) on the penetration of the

injectant into the air stream and jet break-up.

The third area of interest was the behavior of the injected fluid downstream of the step in the region of the combustor.

1.3 Methods of Investigation

Spark and streak shadowgraphs, video tapes and surface flow visualization were employed in the investigations of the jet plume, the main air stream and the downstream behavior of the injectant. The macroscopic behavior of the jet and injectant were observed. Pitot pressure surveys and wall pressures were used to determine the flowfield characteristics in the test section.

1.4 Principal Results

The test section with variable internal geometry and flow control was designed and successfully operated. Flowfield investigations showed that the test section had uniform transverse velocities except for a boundary layer on the walls. The boundary layer at the location where the liquid was injected was approximately 0.15 in. thick. It was found that the step height and the injector distance from the step had no observable effect on penetration or break-up. Downstream of the jet, a portion of the injectant became attached to the wall of the combustor. This injectant then formed a liquid film on the surface of the combustor wall which was driven upstream, back toward the step face, where it formed large drops which were entrained back into

the air stream. This phenomenon was most pronounced at low penetration levels (i.e. low injectant flow rates).

2.0 EXPERIMENT APPARATUS AND PROCEDURES

2.1 Test Facility

This study was conducted at VPI&SU with a special test section in the supersonic/transonic wind tunnel operated by the Aerospace and Ocean Engineering Department. The wind tunnel normally has a 9 x 9 in. test section area and is of the blowdown type. Throughout this work the stagnation temperature was that of the ambient air (approx. 75°F). The stagnation pressure was regulated by a pneumatically-controlled butterfly valve. During the tests, the stagnation pressure was maintained to within 5% of the mean value of 12 PSIG for a run duration of about 12 seconds.

2.2 Wind Tunnel Test Section

A special test section model was designed and built to perform this work. It had the capacity to control the Mach number of the inlet flow from 0.4 to 0.9 and was equipped with variable internal geometry. See Figure 3 for a view of the test section without side plates. In this model test section, the flow was accelerated up to the test level desired in the converging region of the test section, and the flow then stabilized in the inlet region. Following this, the flow expanded over the step into the "combustor" region of the test section. The inlet Mach number was regulated by a variable area throat at the downstream end of the combustor. The test section was of two dimensional design,

which allows the use of shadowgraph and Schlieren photography to investigate the flowfield.

The test section may be considered as having four distinct regions, which are shown in Figure 3. The Converging Region was fabricated from four streamwise running plates laminated together. The plates were sawed roughly to shape, bolted together, and finished by milling and hand-grinding.

The Inlet section and step face were fabricated from 2 in. thick aluminum plates, bolted together. This assembly was then bolted to the converging section and finished by milling and hand polishing. Wall pressure taps .040 in. in diameter were located as shown.

The Combustor section was made from one aluminum plate 2 in thick. This plate was raised and lowered by means of a 1 in. diameter threaded rod.

The lower section of the Nozzle was fitted to the end of the test section and shaped as shown. The opening of the Nozzle was controlled by a flap located on the upper surface of the test section, positioned with threaded rods and hinged at the leading edge.

The entire assembly was sandwiched between stainless steel laminated side-plates. Large rectangular aluminum plugs were fitted into the side plates, and into these plugs were fitted the windows. By inverting the rectangular plugs and manipulating the windows, the entire combustor and part of the inlet region could be exposed for shadowgraphing of the flowfield.

The movable injectors were constructed and located as described

below. One injector was used at a time; the remaining injector locations were then used as static pressure taps.

2.3 Liquid Injection System

Water was used as a representative liquid injectant throughout the tests, because of convenience and safety. Also, much of the available data on jet injection was for water. Existing work indicated that fluid properties, such as viscosity and surface tension, were not of first order importance for jet penetration and break-up,[15] though this point needs further study and verification. The water was injected transversely to the airstream through the lower wall of the inlet region ahead of the step. Locations of the injectors are shown in Figure 4.

A schematic drawing of the injectant pressurization and regulation system is shown in Figure 5. The liquid was pressurized using commercially bottled nitrogen gas; a regulator attached to the nitrogen bottle maintained the back-pressure at about 250 psi. The fluid was filtered through a 140 micron filter. A pressure transducer and a turbine type flow meter was also in the feed line but not used for this work. A needle valve was used to regulate the flow, and the flow rate was measured with a Rotometer. The flow was turned on and off with a manually switched solenoid valve.

Four of the injectors consisted of interchangeable brass inserts held in the test section with hollow aluminum plugs. Fluid was fed

through these plugs to the injectors. See Figure 6(a) for a section view. The upper "O" ring was used to allow height adjustment of the injector insert. All injectors were mounted flush with the inlet plate surface. The lower "O" ring in Figure 6(a) sealed the insert to the aluminum plug.

Because of physical constraints, a small injector was used at the 0.5 in. location. For this injector a 0.188 in. diameter hole was drilled through the inlet plate, a brass insert was pressed in from the top and a 0.188 in. outside diameter stainless steel supply tube was pressed in through the bottom. See this arrangement in Figure 6 (b). All injectors used had 0.040 in. injection port diameters.

The two types of injectors were found to behave slightly differently, therefore the data from the two injectors were not directly compared to each other. The results from each injector were compared to control data taken from the same injector with no step (i.e. h = 0) in the test section. The injector located at 0.5 in. produced a more coherent jet with a slight increase in penetration. This behavior prompted a study to determine the effect of nozzle length and inlet geometry on jet formation. The injector investigation was done in still air and was of a qualitative nature, and the results will be discussed later.

2.4 Instrumentation

A vertical traverse mechanism was installed through the top of

the test section. A multi-turn potentiometer gave location, and two rakes were used with this device. A five probe total pressure rake was used to measure flow uniformity in the vertical and transverse direction. A single probe total pressure rake was used to determine the boundary layer thickness. Figure 7 shows general dimensions of these rakes. Photographs of the total pressure rake may be seen in Figure 8.

All pressures were measured with a 48 position Scanivalve. The Scanivalve was equipped with 19 pressure holding tanks, so that 19 pressures could be taken simultaneously during a run. The 19 pressures were then recorded on a strip chart after a test run was completed.

The total pressure in the plenum chamber was continuously monitored and recorded during each run using a strain-gauge type pressure transducer. Also measured in the plenum chamber was the total temperature of the air using a thermocouple. All pressures, the temperature and rake position were recorded on strip chart recorders. See Table 1 for a description of all the instruments used.

2.5 Photography

Four types of photographing and visual recording techniques were used for this work:

1) Streak shadowgraphs (10^{-3} sec.),

2) Spark shadowgraphs (10^{-8} sec.),

3) Direct photographs, and

4) Video tapes.

The camera and lens arrangement were the same for both the streak and spark shadowgraphs, but the light source varied. Figures 9 and 10 show sketches of the set-ups. The streak shadowgraphs were back-lighted photographs which were of long enough exposure to yield the time integrated shape of the water plume and some visual, qualitative information about the concentration of the injectant in the air. For these photographs, a Vivitar photographic flash unit (10^{-3} sec.) was used as the light source. It was used at full intensity and placed in a light proof container with a 1/8 in. aperture through which the light could pass. The light intensity was reduced through photographic filters. The light source was placed at the focus point of a 10 inch parabolic mirror, which was used to obtain a parallel light beam. This beam passed through high-quality optical windows in the side plates of the test section and was focused on the optical plane of the camera. A lens was not mounted in the camera itself but in front as shown. The room was darkened during the tests. The camera had a focal plane shutter which was syncronized with the flash unit, but the camera remained open a relatively long time, so that the flash duration of 10^{-3} seconds was the effective exposure time of the film. The film was Polaroid Type 55 positive/negative black and white film (ASA 50).

The spark shadowgraphs were of much shorter exposure, 15 nanoseconds. The Nanopulser light source was mounted immediately behind the test section, and the light passed directly through the tunnel into

the camera. For the spark shadowgraphs, the focal plane shutter was left open, and an iris type shutter at the front of the camera was used. The diameter of the light source restricted the field of the photographs to 1.3 in. High speed film was required for this work because of the short flash exposure time and low light intensity, so Polaroid Type 57 film (ASA 3000) was used. The spark shadowgraphs were of an instantaneous or stop-action nature.

Type 57 film was also used for direct photos, which were illuminated with two flood lights. The two flood lights were also used for video tape recordings, which were done with a Sony AVC-3400 video camera equipped with a 12-64 mm, F2.8 zoom lens, with Scotch 0.5 in. high-energy video tape.

2.6 Experimental Procedure

Test section calibrations and flowfield investigations were performed using the wall ports and the Scanivalve to measure static pressures along the lower surface of the test section. The scanning rate was 4 ports per second, so that 12 seconds of steady state run time were required to scan all 48 ports. The pressure distribution across the section was found using two rows of static pressure ports and the total pressure rake.

Boundary layer measurements were made by plotting Pitot pressure and boundary layer probe position simultaneously on a strip chart.

Most of the runs were made to take shadowgraphs, and these runs

were made in the following manner. The wind tunnel was started, and, immediately afterward, the water injection was initiated and regulated by hand to the desired flow rate. After the air and water velocities were stabilized, the camera timer was started. This timer operated the camera, flash, Scanivalve and event markers on the strip chart. After the photograph was taken, the injection was stopped, but the wind tunnel was allowed to run a few seconds longer to clear out any accumulated water.

The tests where a video recording was made were run similarly. No timer was used because the runs were monitored continuously. For most of these runs the water injection rate was started high or low and decreased or increased continuously by hand during the run. The instantaneous injection rate was read from the Rotameter and recorded vocally on the sound track of the video tape.

For the oil-drop surface flow visualization tests, two media were used: a commercial product called "STP" and castor oil. A powered dye was used with both media. The medium was dripped on a grid drawn on the combustor region surface. The wind tunnel was operated until the oil drops began to run, thus the oil was unavoidably exposed to the transient start-up and shut-down conditions of the flowfield. The less viscous castor oil was used only in the low surface velocity region immediately behind the step.

3.0 RESULTS

3.1 Results and Discussion

3.1.1 Test Section Flow Without Injection

The results of two total pressure surveys across the test section flow without injection may be seen in Table 2. For these surveys the step height was 1.0 in., the most extreme case investigated in this work. The pressure surveys show that a uniform flowfield was produced in the test section. The X, Y & Z distances listed correspond to the coordinate system shown in Figure 11. For Y dimensions of 0.5 in. and greater, the Pitot pressure was found to be as much as 2% greater than the Pitot pressure in the plenum chamber ($P_{o,\infty}$); this error was within the measurement capabilities of the equipment used for the survey.

Static wall pressure surveys were made for different step heights, and the results of three of these may be seen in Figure 12. The pressures were taken along the center of the lower wall of the inlet and combustor region. The pressure ports are shown as dots in Figure 3 and as crosses in Figure 4. The wall pressure tests also showed a generally uniform flowfield for the zero step height case.

The static pressure survey for the 1.0 in. step height showed that the pressure increased toward the downstream end of the combustor region and reached a plateau about 12 - 14 in. behind the step. As was found by Drewry [19] for an axisymmetric model, the maximum wall

static pressures occurred well downstream of the flow reattachment point. This point was determined from the flow visualization photographs shown in Figure 13 and 14. Figure 13 is the result of an oil drop test for a 1.0 in. step height where the oil drop array was a 1.0 in. by 1.0 in. square grid. The upper photo shows the oil drop array before exposure to the air flow. After the test was run, the lower photograph was made. Near the center of this photograph an area where no oil crossed may be seen, indicating that the surface flow proceeded away, upstream and downstream, from this region. This was between 6 and 7 in. and indicated that the stagnation point of the flow was in this area. Figure 14 is similar to Figure 13 except that a 0.5 in. by 0.5 in. array was used. This test showed the reattachment point to be between 6 and 6.5 in. Knowing that the distance that the oil drops ran was a function of surface velocity, it could be seen from these tests that the flow velocity decreased significantly near the step.

In order to observe this low velocity region more closely, the test depicted by Figure 15 was made using a less viscous oil (castor oil). It may be observed from this photograph that the surface flow was downstream (towards the nozzle) across the line of oil drops which were 0.5 in. from the step base, and that the surface flow was upstream (towards the step) 1.0 in. from the step base, so that a "rear" line of stagnation existed on the combustor surface between 0.5 in. and 1.0 in. downstream of the step base. Also, it may be seen that the flow near the step base was not two dimensional, particularly near the walls of the test section. Because of this, the stagnation

line was not straight but did appear to be symmetrical about the centerline of the test section. Videotapes were made encompassing the injection port, the step and the step base region of the combustor surface during tests where liquid was injected. From the tapes the presence of this additional stagnation line was also indicated, since some injectant accumulated about it. These results will be presented in detail later.

3.1.2 Shadowgraphs of Liquid Jets

Figures 16 through 21 are streak shadowgraphs of the liquid jet in the Mach 0.6 flowfield where the air flow is from left to right. As mentioned in Section 2.5, these photographs show the time integrated shape of the injectant jet. Figures 16 through 18 are results of control tests where no step was used. The $\bar{q}$ for the tests throughout this work were computed without including the discharge coefficient. As mentioned previously, the two types of injectors had slightly different penetration results, which were due to a slight discharge coefficient variation. Comparing figure 16(a) with 17(b) it can be seen that the jet in Figure 17(b) is more coherent near the injector and penetrates farther into the flowfield. Similar comparisons between Figures 16(b) and 18(a) and between Figures 17(a) and 18(b) show similar results. Because of this injector behavior, the results of later tests where a step was included were compared directly to the control (zero step case) photographs taken at the same location only. Also

because of this phenomenon, a short qualitative study was made in still air to determine the effect of nozzel length and inlet geometry on jet formation. Results indicated that the distance to break-up decreased with increasing velocity, also the longest break-up lengths were produced by injectors with low length to diameter ratios. At high velocities, sharp inlet nozzles tended to slightly increase the distance to break-up and to make the jet more coherent near the injector.

Figures 19, 20 and 21 are results of tests run at a 0.5 in. step height. As in Figures 16 through 18 the air flow is from left to right at Mach 0.6. By comparing these and similar photographs to the photographs of Figures 16 through 18, no change in penetration could be observed due to the presence of the step or the value of the step height. Thus, penetration was found to be only a function of $\bar{q}$ and injector geometry, and the results of Ref. (3) for injection through a flat plate model can be applied in this geometry as well. Injectant drops may be seen to be forming on the windows in the separation zone behind the step, and they are most pronounced at the lower $\bar{q}$'s. More will be said about this process later.

A qualitative study of jet break-up and instantaneous plume structure was carried out. Spark shadowgraphs taken for this study are shown in Figures 22, 23, & 24. The flow is from left to right at Mach 0.6 as it was for the streak shadowgraphs; the $\bar{q}$, step height and injector distance are given. Two qualities are apparent from the shadowgraphs: the shape of the leading edge of the jet and the

density of the jet. As was found by the investigators in Reference 1, the waves on the leading edge of the jet are of shorter length for higher $\bar{q}$. Also, the jet breaks up and disperses farther down stream of the injector for the higher $\bar{q}$.

The simplest explanation for the lack of influence of step height or location (related to the injector) on penetration is as follows. First, the changes in gas flow direction due to the presence of the step were rather small. For the 1.0 in. step height, the reattachment point was 6 - 6.5 in. downstream, so the maximum streamline slope was of the order of 1:6. Second, the inertia of the liquid clumps and droplets was large compared to the gas. The initial turning of the jet occurred close to the injection point (See Figs. 16 - 21), and the jet plume was then essentially horizontal. Taken together, these two factors indicate that the gross behavior of the jet plume is largely unaffected by the presence of the step.

3.1.3 Injectant Accumulation Behind the Step

It was observed that injectant accumulated on the wall in the recirculation region behind the step and the amount was strongly affected by $\bar{q}$. At low $\bar{q}$, injectant accumulation became substantial. This can be seen by comparing Figures 22(a), 22(b) and 23(a), and noticing the increase in accumulation on the windows with decreasing $\bar{q}$ in the step-base region. Similar behavior is noted on comparing 23(b), 24(a), and 24(b). Also this phenomenon was observed by simply

watching the flow on the combustor surface behind the step during the tests. Later, video tape recordings were made in order to further observe the injectant behavior in the step base region, and in the recirculation zone. A photograph taken from a video tape may be seen in Figure 25, where the test conditions were: $\overline{q}$ nominally equal to 2.0, h = 1.0 in. and d = 1.0 in. It was observed that the injectant formed puddles about the stagnation line on the combustor surface. Further study of the tapes and photograph in Figure 25, showed that the liquid surface film did not extend all the way back to the interior step corner. There was a film-free zone extending about 0.5 to 1.0 in. out from the step base, this is roughly the area influenced by the imbedded vortices (See Fig. 2). Also, it was evident from these tapes and tapes taken further downstream in the combustor region that most of the injectant accumulating on the combustor surface came from the flow reattachment point. The injectant flowed along the combustor surface as a thin film and as small streams, away from the reattachment point both upstream towards the step and downstream towards the nozzle. A small amount of injectant would adhere to the inlet surface behind the injection port and form a thin narrow film which would go over the step into the combustor region. This flow rate was small compared to the injectant flow rate from the reattachment point.

The puddles of injectant would increase in size until they apparently attained enough height to be entrained into the flow in the recirculation zone. When this happened, large clumps of fluid were broken away up into the flow. The accumulation of the injectant on

the combustor surface is significant in that it may contribute to unsteady, incomplete and smoky combustion in the actual ramjet engine. No suitable method for measuring the mass accumulation was devised during this investigation, therefore no quantified results are available in this area.

3.2 Conclusions

The test section and injection system functioned well; the test section produced a spanwise uniform inlet flow without injection. Pressure surveys were made of the test section flowfield and various types of photographs were used to investigate the injectant behavior. Surface flow visualization tests were also made in order to understand the flowfield more fully. The optical techniques employed in the investigation displayed the features of the jet plume and the interaction of the jet plume with the flowfield. Penetration and break-up of the jet were not observed to be a function of the step height or distance from the injector to the step.

These studies showed large accumulations of injectant behind the step on the combustor surface. Such surface films and the resulting large drops of injectant will have effects on efficiency and smoke production in ramjet engines using this type of combustor. The amount of injectant accumulation was found to be primarily dependent on jet penetration, i.e. the ratio of the dynamic pressure of the injectant jet to the dynamic pressure of the airstream for these investigations.

During this work, it became evident that some simple, direct method for measuring injectant accumulation rate should be developed. With that, areas for future work include: correlation of injectant accumulation with step location and height and to the thickness of the boundary layer through which the fluid is injected. It may be possible to reduce accumulation by extracting injectant from the combustor wall. Alternatively, contouring the interior corner of the step to eliminate the low surface velocity zone may reduce injectant accumulation without adversely affecting the flame holding property of the step.

REFERENCES

1. Belding, J., and Coley, W., "Integral Rocket/Ramjets For Tactical Missiles," Astronautics and Aeronautics, Volume 11, Number 12, pp. 20 - 26, December 1973.
2. Nelson J. and Strand, G., "Propulsion Lab Shaping Future Designs," Aviation Week and Space Technology, Volume 110, Number 5, pp. 235 - 237, January 29, 1979.
3. Schetz, J., McVey, W., Padhye, A., Munteanu, F., "Studies of Transverse Liquid Fuel Jets in High-Speed Air Streams," AFOSR-TR-76-1168, July 1976.
4. Rayleigh, Lord, Proc. London, Math. Soc., 104, 1878.
5. Rayleigh, Lord, Phil. Maq., 34, 153, 1892.
6. Mayer, E., "Theory of Liquid Atomization in High Velocity Gas Streams," ARS Journal, pp. 1783-1785, December 1961.
7. Weiss, C. and Worsham, C., "Atomization in High Velocity Air Streams," ARS Journal, Volume 29, Number 4, p. 252, April 1959.
8. Clark, B., "Break-up of a Liquid Jet in a Transverse Flow of Gas," NASA TN D-2424, August, 1964.
9. Adelberg, M., "Mean Drop Size Resulting From the Injection of a Liquid Jet into a High Speed Gas Stream," AIAA Journal, Volume 6, Number 6, pp. 1143-1147, June 1968.
10. Morrell, G. and Povinelli, F., "Breakup of Various Liquid Jet by Shock Waves and Applications to Resonant Combustion," NASA TN D-2433, August 1964.

11. Ranger, A. and Nicholls, J., "Aerodynamic Shattering of Liquid Drops," AIAA Journal, Volume 7, Number 2, pp. 285-290, May 1969.

12. Yates, C. and Rice, J., "Liquid Jet Penetration," Research and Development Programs Quarterly Report, U-RQR/69-2, Applied Physics Lab., Johns Hopkins University, 1969.

13. Sherman, A., "Investigations into Breakup of Liquid Sheets and Jets in a Supersonic Gas Stream," Ph.D. Thesis, University of Maryland, 1969.

14. Joshi, P. and Schetz, J., "Effect of Injector Shape on Penetration and Spread of Liquid Jets," AIAA Paper Number 74-1156, AIAA Journal, Volume 13, Number 9, pp. 1137-1138, September 1975.

15. Nejad, A., Schetz, J., and Jakubowski, A., "Mean Droplet Diameter Resulting from Atomization of a Transverse Liquid Jet in a Supersonic Air Stream," Air Force Office of Scientific Research/NA, AFSOR-TR-79-0004, VPI-Aero-089, November 1978.

16. Abbott, D., and Kline, S., "Experimental Investigation of Subsonic Turbulent Flow Over Single and Double Backward Facing Steps," Journal of Basic Engineering, pp. 317-325, September 1962.

17. Kanqovi, S. and Page R., "Subsonic Turbulent Flow Past a Downstream Facing Annular Step," American Society of Mechanical Engineers, paper 78-WA/FE-15, December 1978.

18. Drewry, J., "Fluid Dynamic Characterization of Sudden-Expansion Ramjet Combustor Flowfields," AIAA Journal, Volume 16, November 4, pp. 313-319, April 1978.

19. Drewry, J., "Characterization of Sudden-Expansion Dump Combustor Flowfields," Air Force Aero Propulsion Laboratory, AFAPL-TR-76-52, July 1976.

Table 1 - Instrumentation

Type of Instrument	Brand and Model Number	Use
Strip Chart	Hewlett Packard Model 710013 with 17501A Modules	To record all pressures and Total Temperatures
Multiple input pressure Transducer	Scanivalve, Inc. Mode J	To measure all pressures in test section
Pressure Transducer	Fredric Flader Type PSH3 Ser.# 428	Total pressure in Plenum Chamber
Thermocouple	Omega Brand, Alloy Type T (copper - constahtine) Thermo Couple	To sense total temp. in Plenum Chamber
Thermocouple Module	Hewlett Packard Model 17502A Temperature Module	To calibrate and record Thermocouple Output
Flow-Meter	Brooks Rotometer Model 1231-1110 Ser.No. 6408-6987/1	To measure injectant flow rate
Lens	Dailmeyer Pentac 240738 f.ℓ. = 8" F 2.9	Shadowgraphs
Flash Unit	Vivitar Auto-Thyrister Model 283	Light source for streak shadowgraphs

Table 1 - Continued

Type of Instrument	Brand and Model Number	Use
Strip Chart	Hewlett Packard Model 710013 with 17501A Modules	To record all pressures and Total Temperatures
High Speed Flash Unit	Xenon Model 437A Nanopulser	Light source for spark shadowgraphs
Camera	B & S View Camera	Shadowgraphs
Shutter	Graflex 1000	Spark Shadowgraphs

Table 2. Results of Total Pressure Survey of Test Section, Mach 0.6

X Inches	Y Inches	TOTAL PRESSURE RATIO $P_o/P_{o\infty}$				
		Z=-1.5"	Z=-0.5"	Z=-0.0	Z=1.0"	Z=2.0"
-0.5	0.03	0.921	0.921	0.924	0.926	0.928
-0.5	0.5	1.005	1.005	1.005	1.007	1.010
-0.5	1.0	1.006	1.006	1.006	1.007	1.007
-0.5	1.5	1.010	1.010	1.007	1.008	1.007
-0.5	2.0	1.005	1.005	1.005	1.005	1.005
-0.5	2.5	1.005	1.005	1.003	1.003	1.003
0.75	0.0	0.923	0.952	0.956	0.931	0.884
0.75	0.5	1.007	1.004	1.006	1.002	1.002
0.75	1.0	1.007	1.007	1.007	1.007	1.007
0.75	1.5	1.010	1.010	1.010	1.010	1.010
0.75	2.0	1.020	1.020	1.019	1.019	1.019
0.75	2.5	1.005	1.005	1.005	1.005	1.005

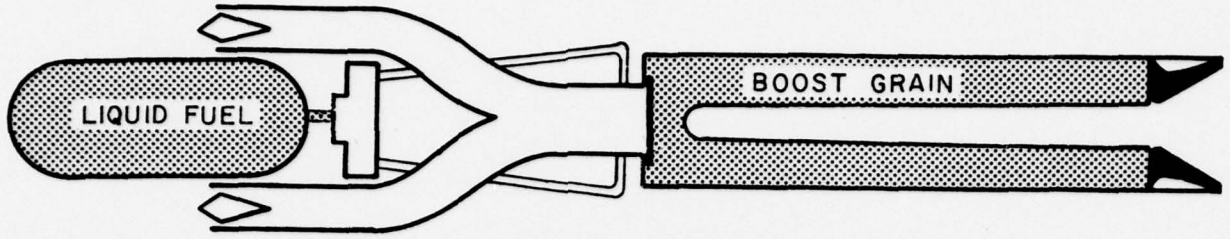

ROCKET BOOSTER PHASE

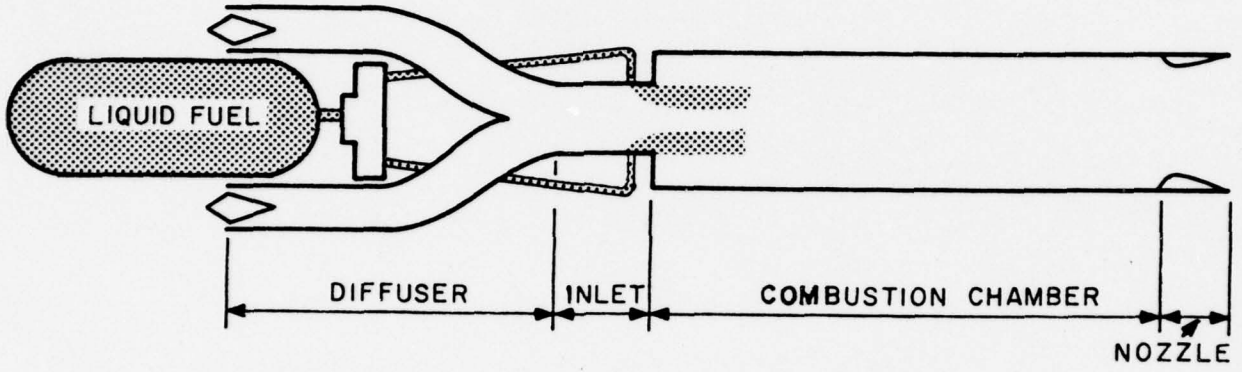

LIQUID FUEL RAMJET SUSTAINER PHASE

Figure 1. Liquid Fuel Integral Rocket/Ramjet

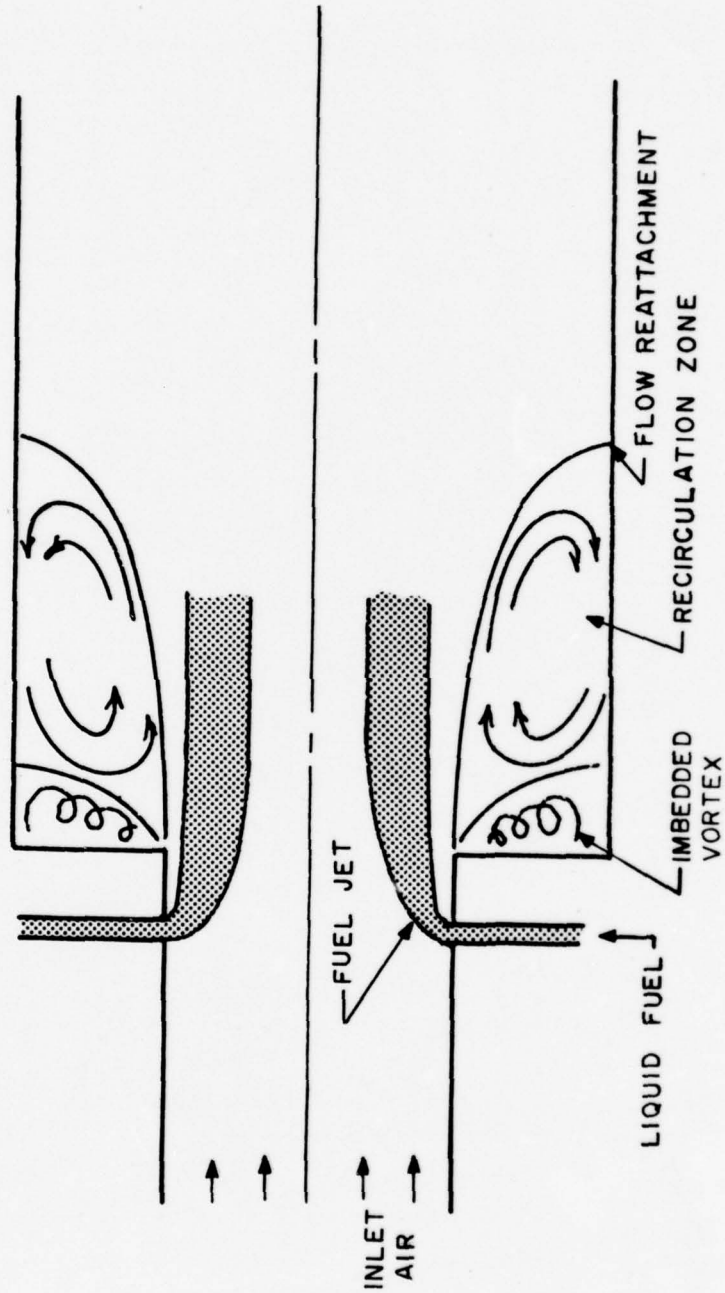

Figure 2. "Dump " Combustor

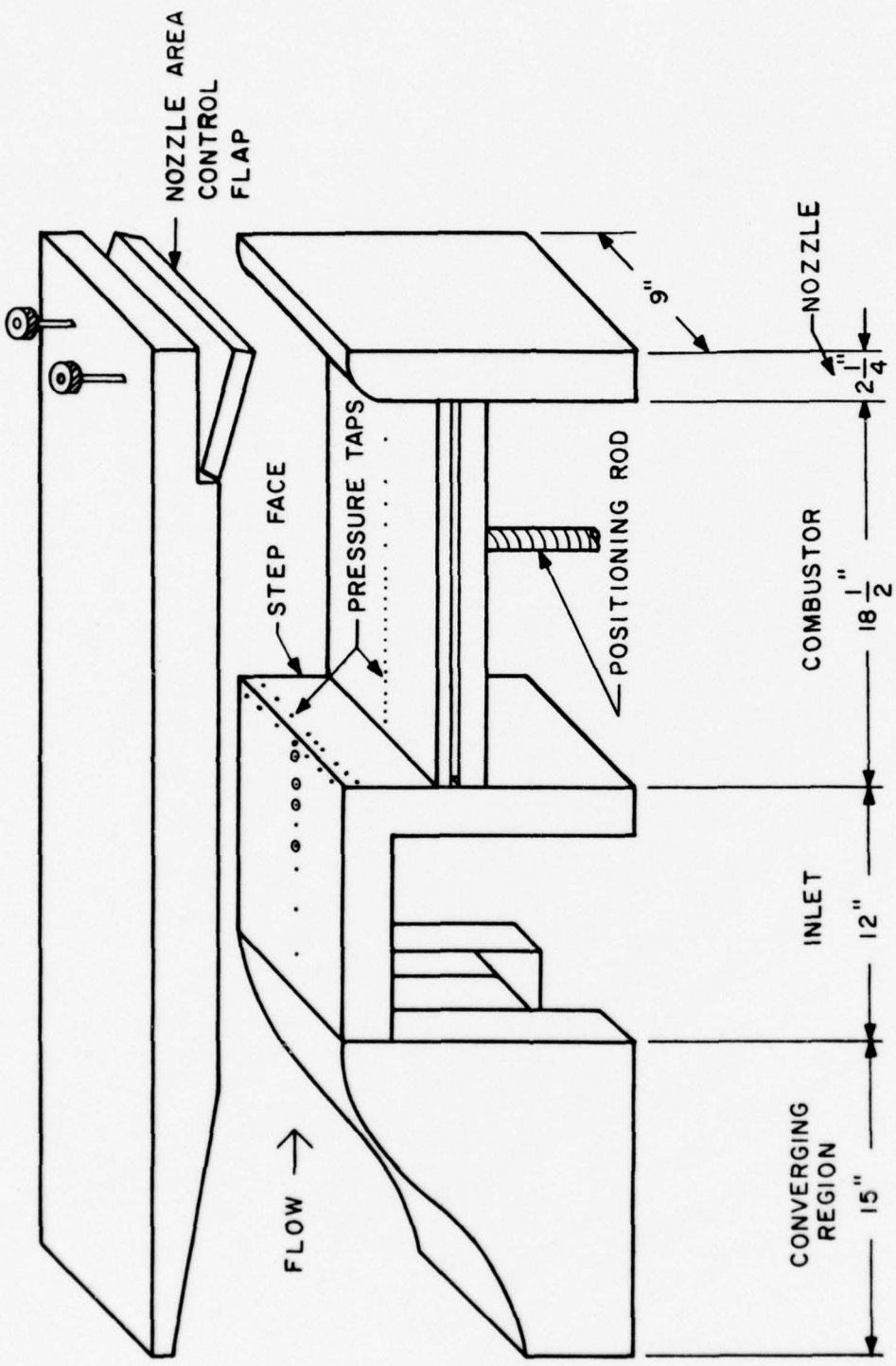

Figure 3. Test Section

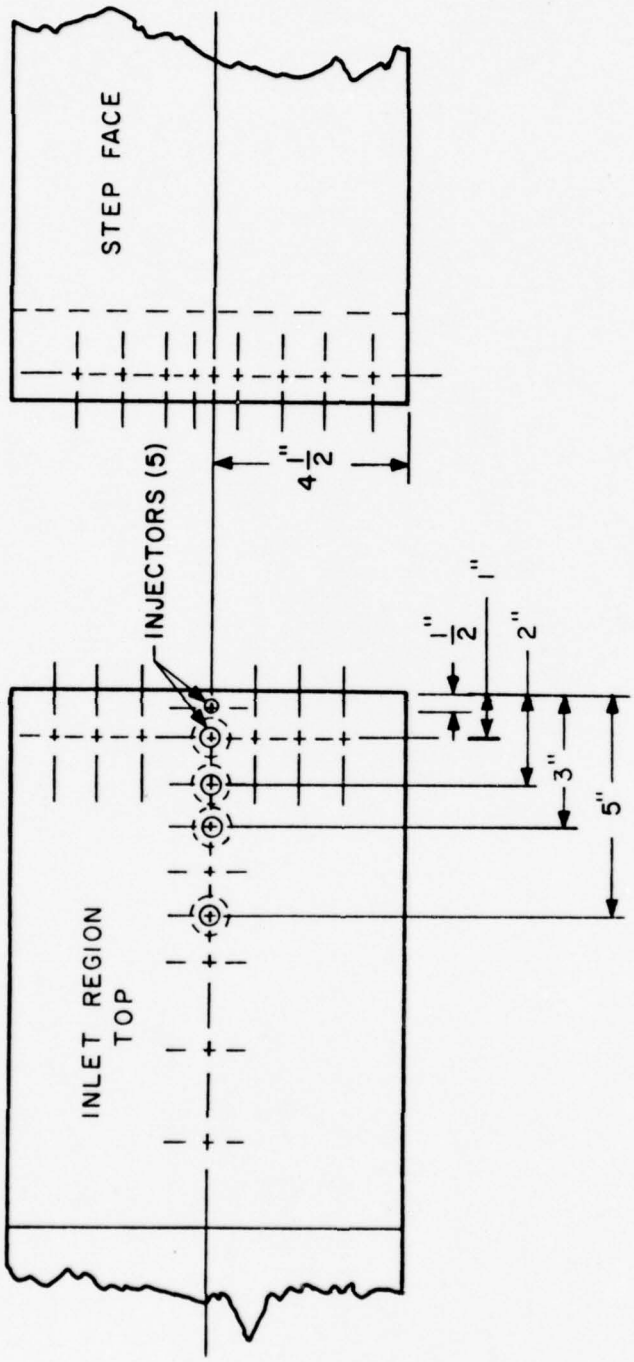

Figure 4. Injector Locations

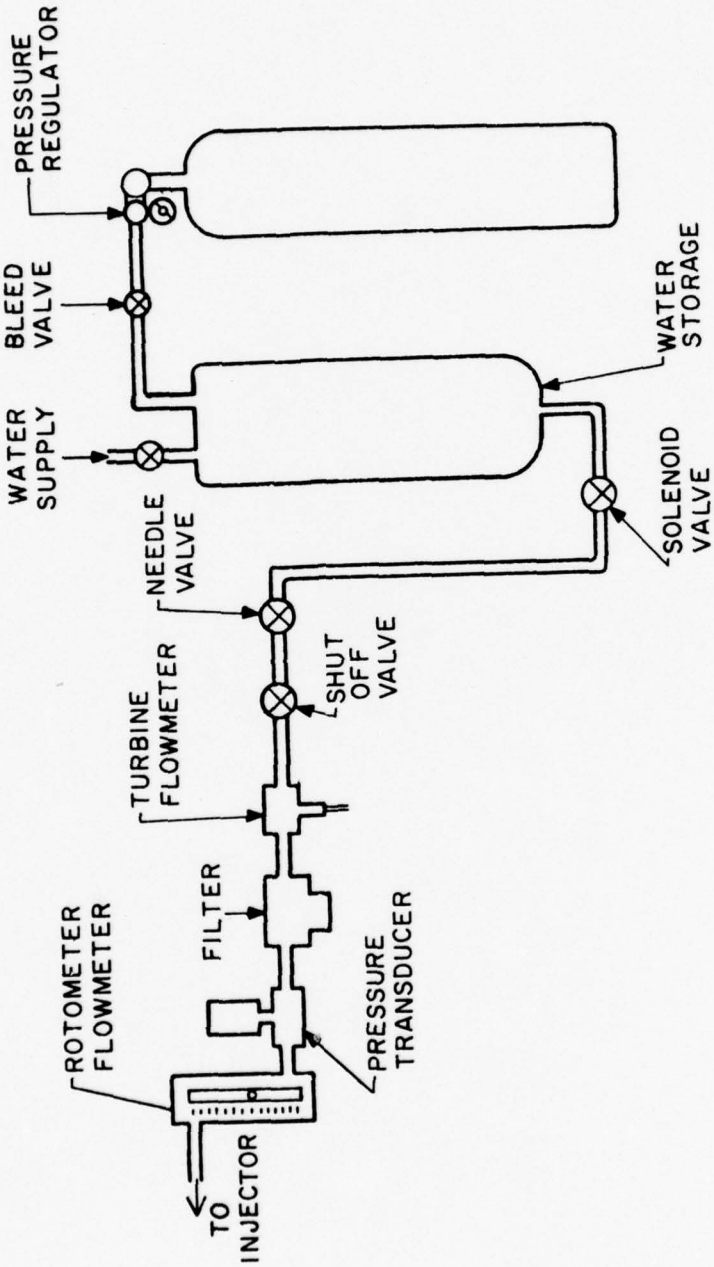

Figure 5. Liquid Injection System

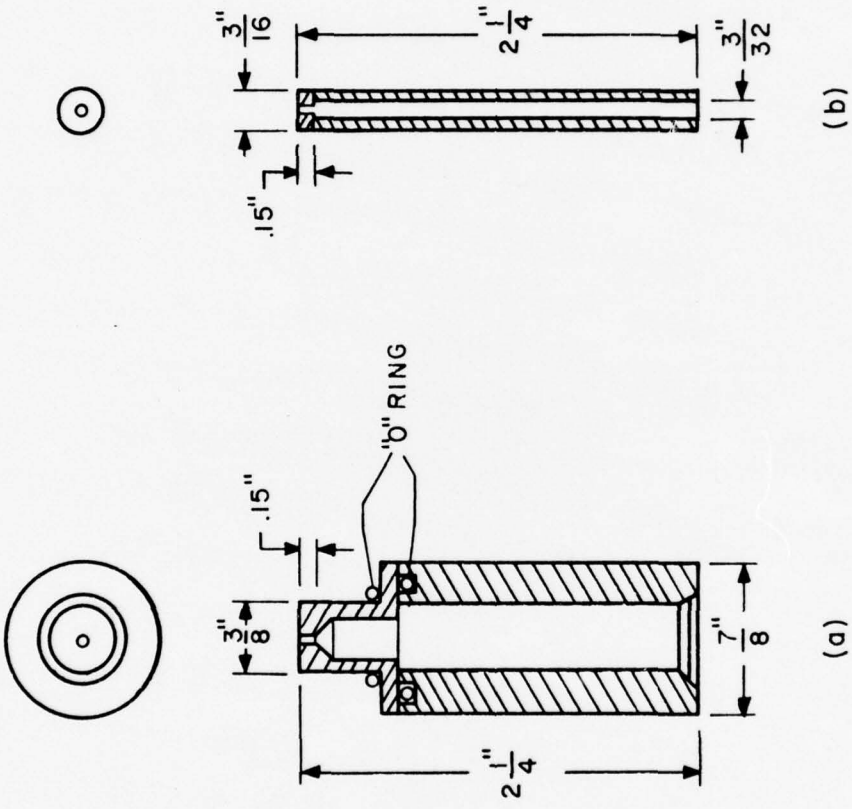

Figure 6. Type of Injector

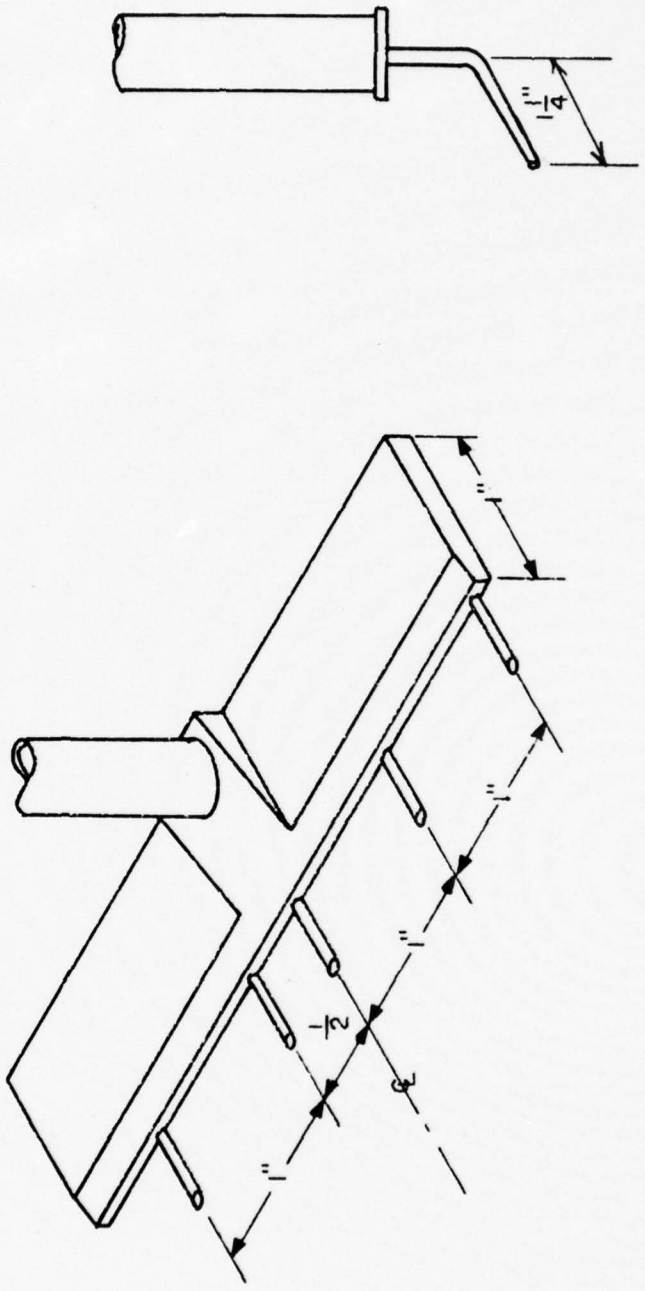

Figure 7. Pressure Survey Rake Details

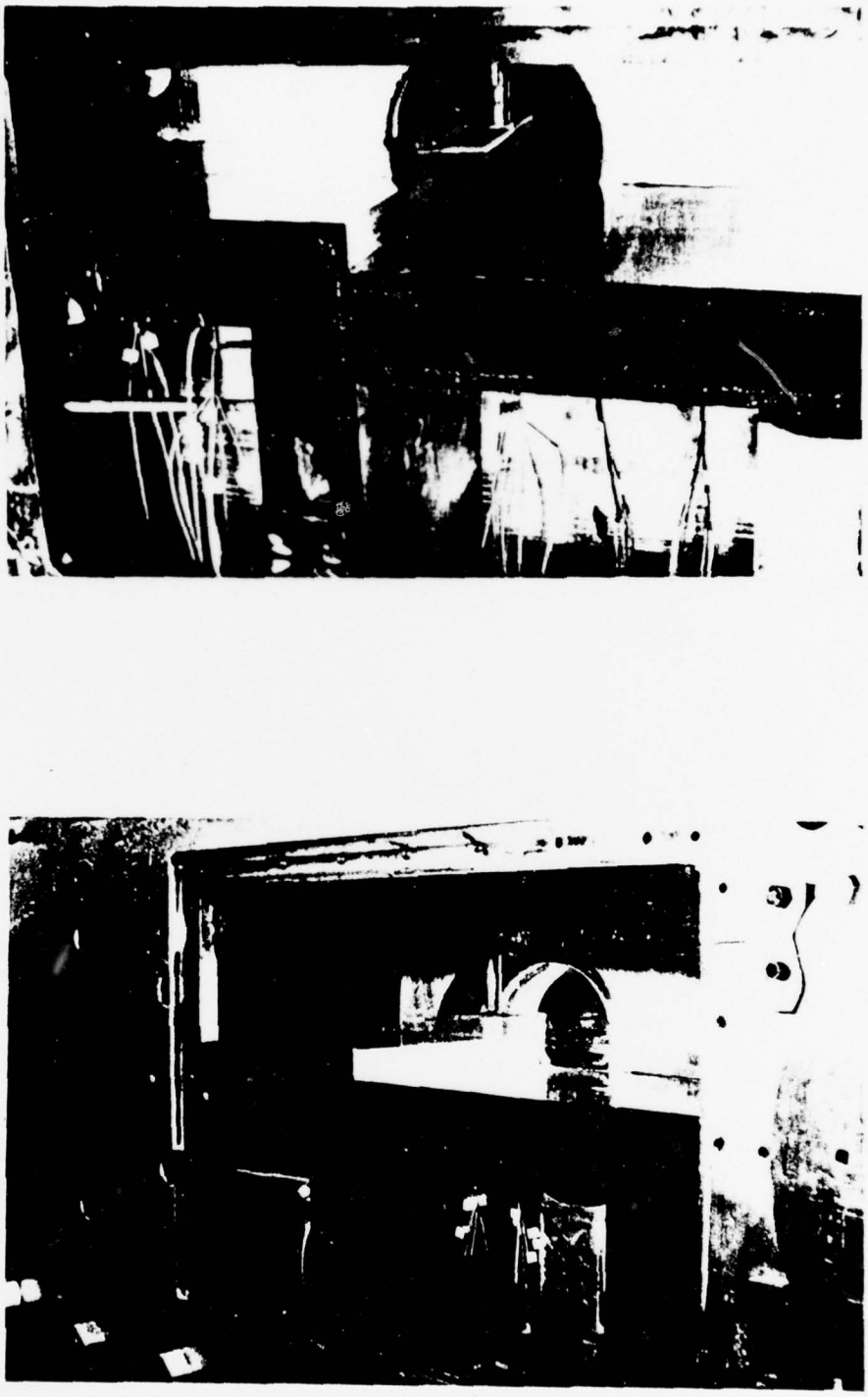

Figure 8. Pressure Survey Rake in Place

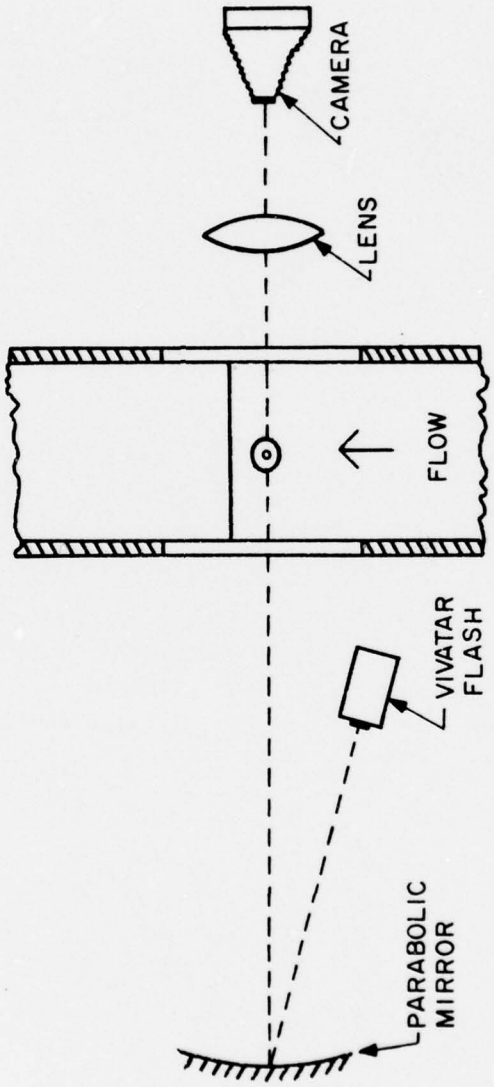

Figure 9. Schematic Sketch of Streak Shadowgraph Set-Up

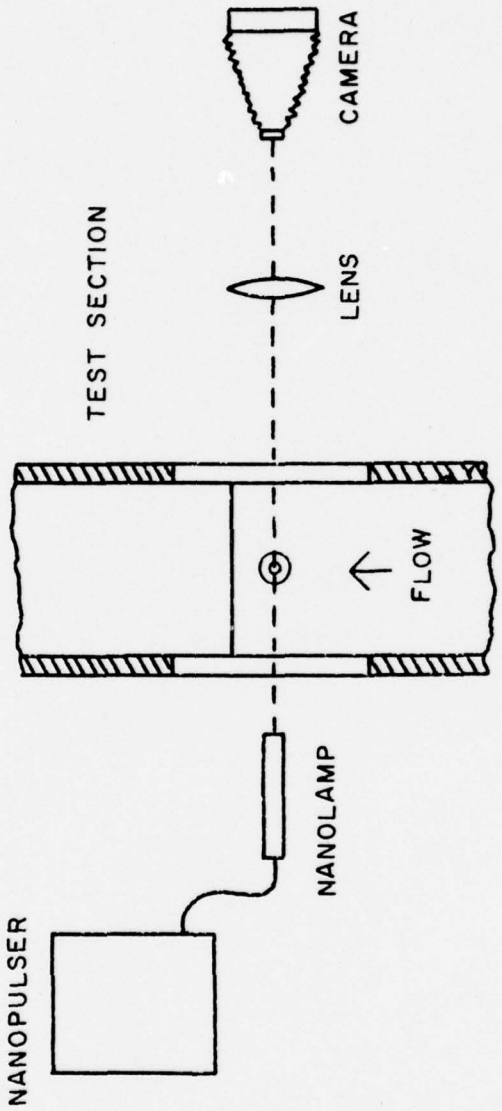

Figure 10 Schematic Sketch of Spark Shadowgraph Set-Up

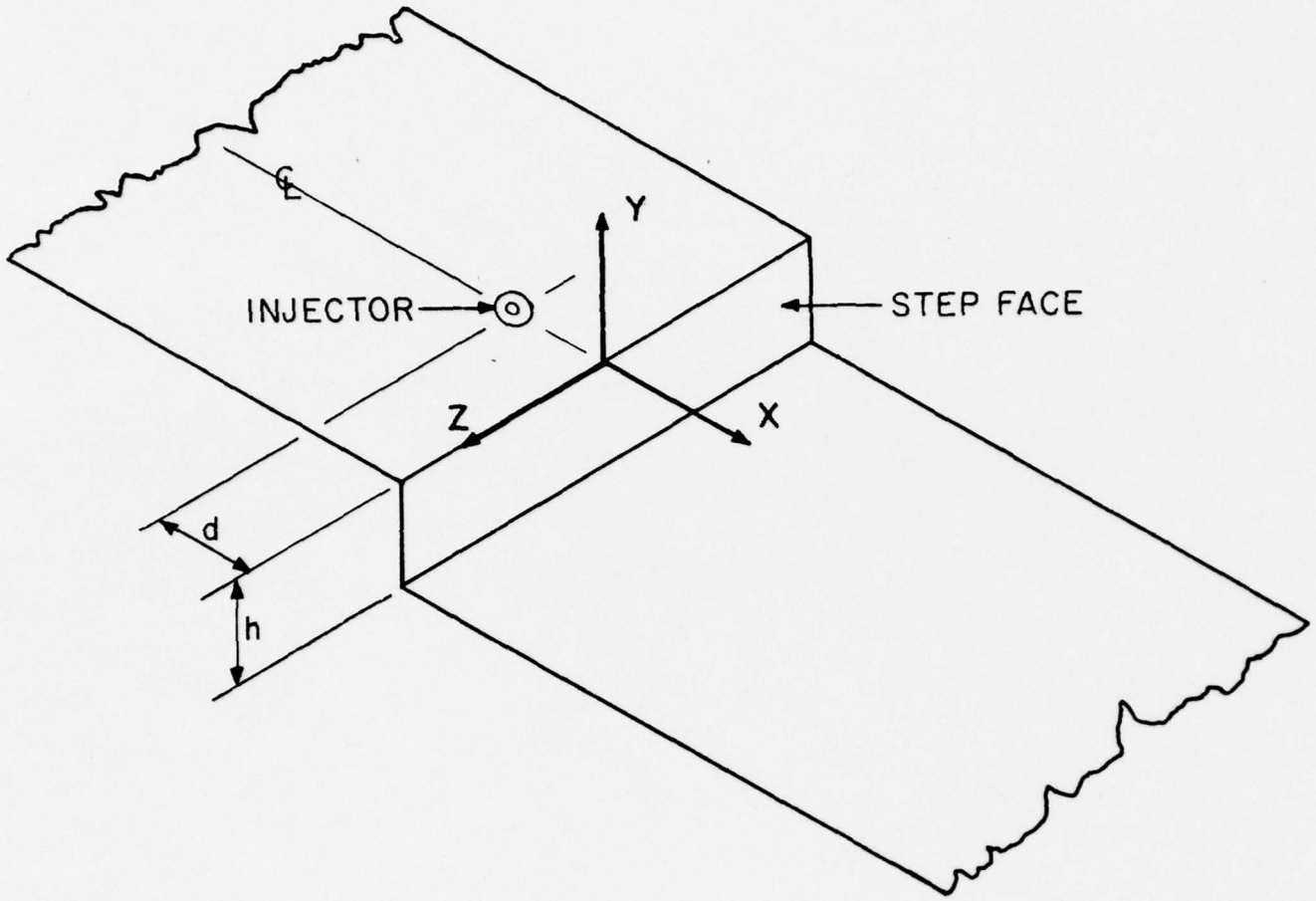

Figure 11. Test Section Coordinate System and Injector Location Dimensions

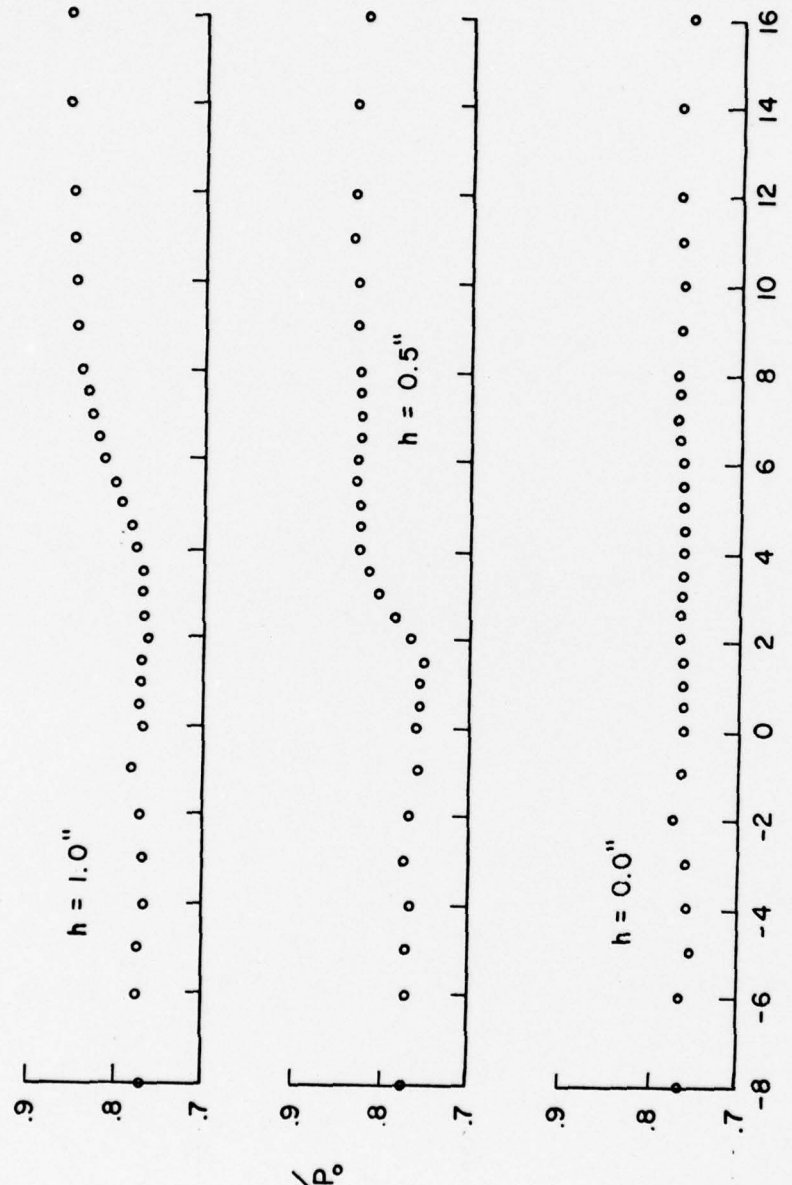

Figure 12. Results of Static Pressure Survey

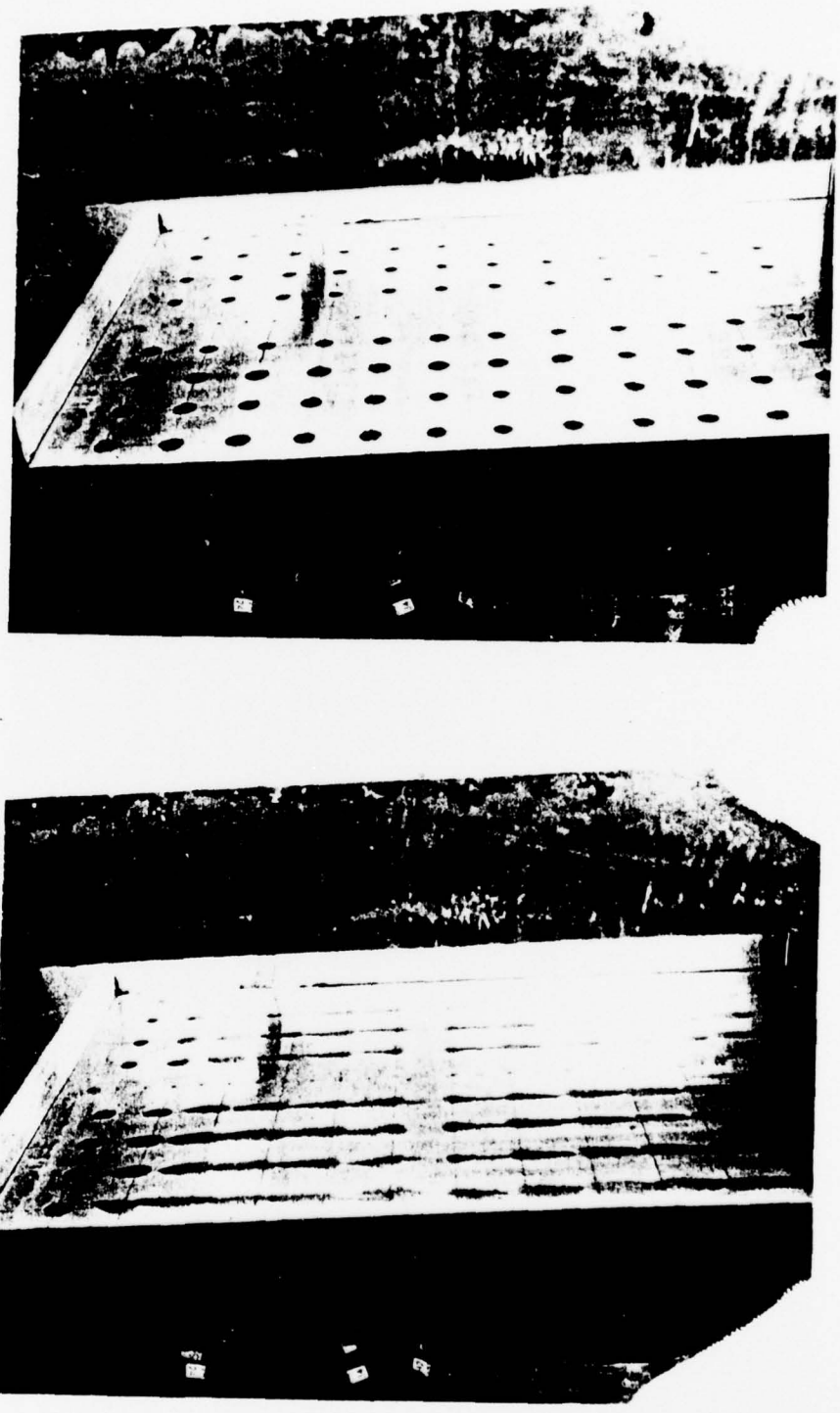

Figure 13. Surface Flow Visualization Test (STP)

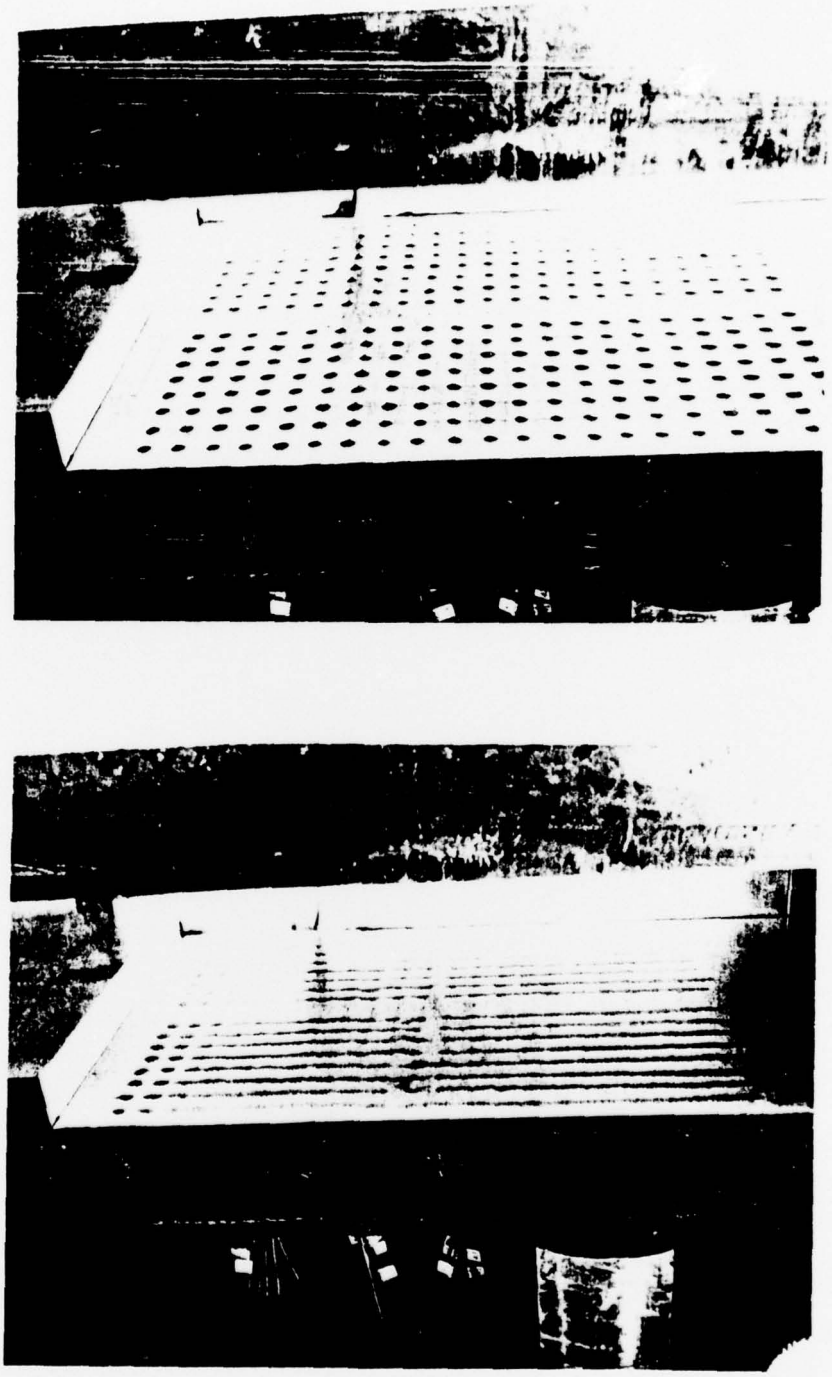

Figure 14. Surface Flow Visualization Test (STP)

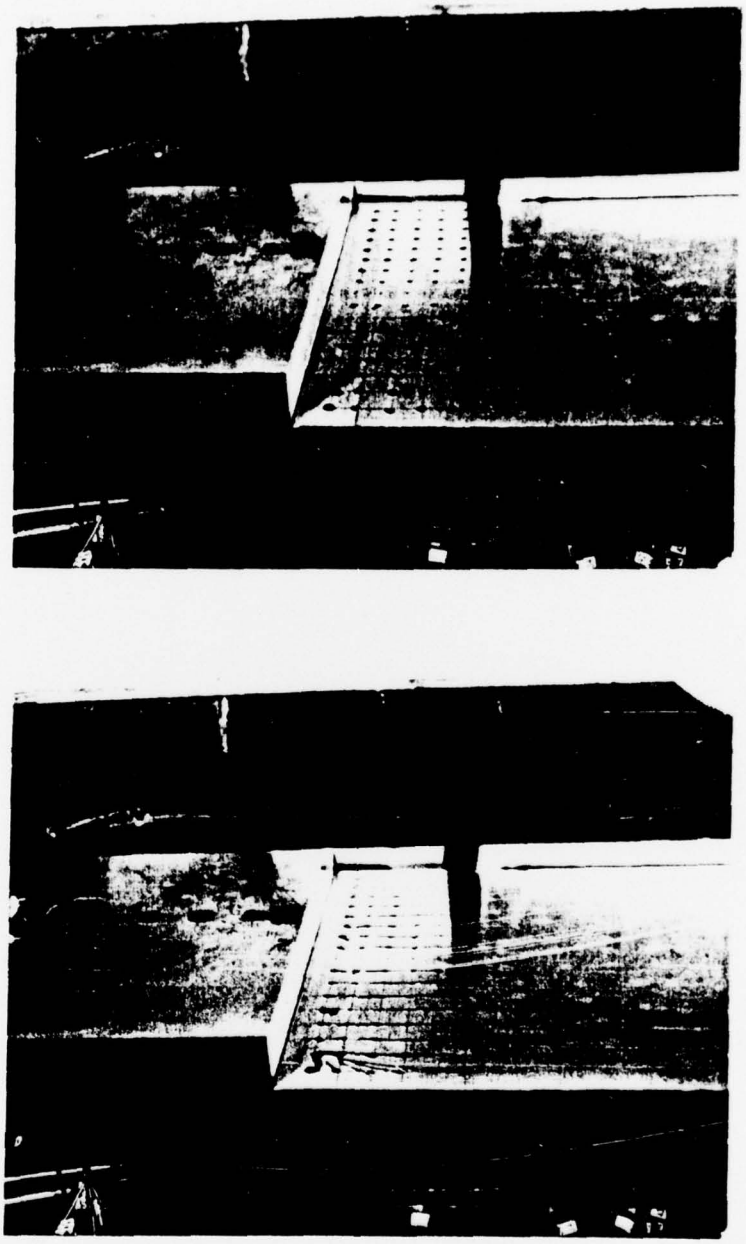

Figure 15. Surface Flow Visualization Test (Castor Oil)

$\bar{q}$=10.2
h=0.0
d=1.0

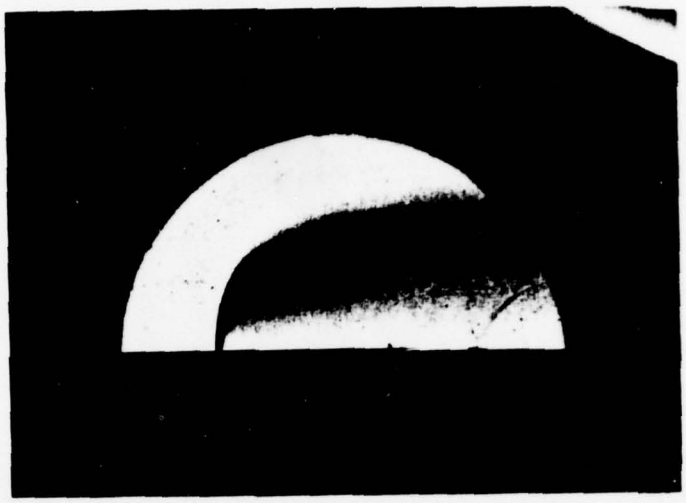

$\bar{q}$=5.07
h=0.0
d=1.0

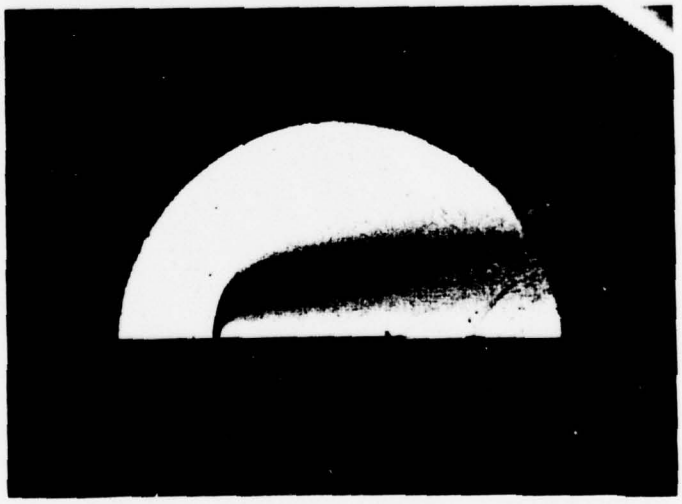

Figure 16. Streak Shadowgraphs of Injection Jet

$\bar{q}$=2.07
h=0.0
d=1.0

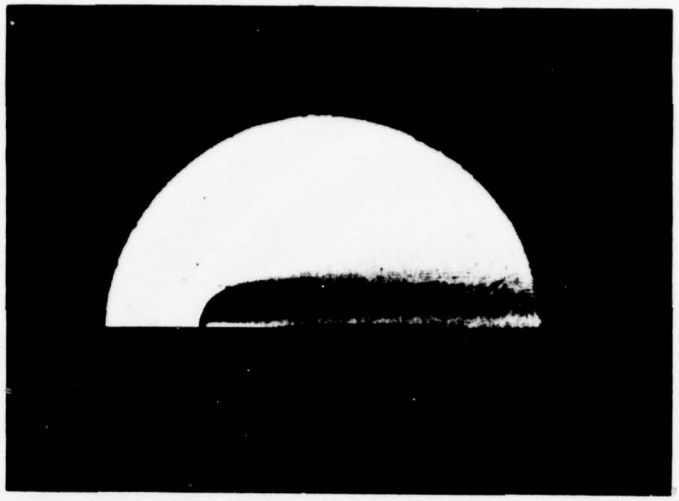

$\bar{q}$=9.97
h=0.0
d=0.5

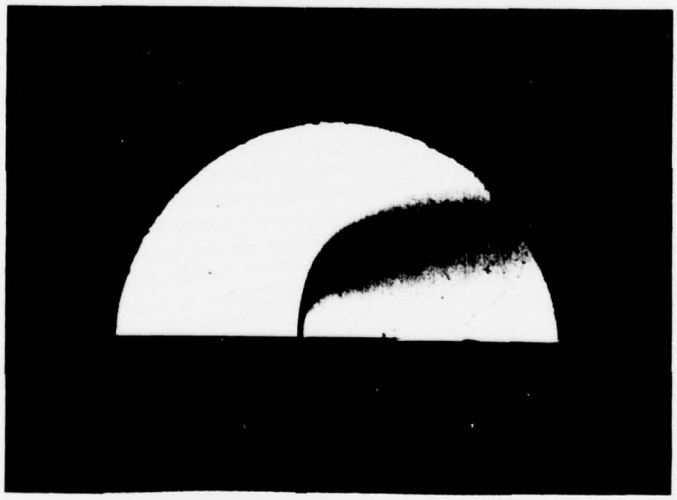

Figure 17. Streak Shadowgraphs of Injection Jet

$\bar{q}$=4.97
h=0.0
d=0.5

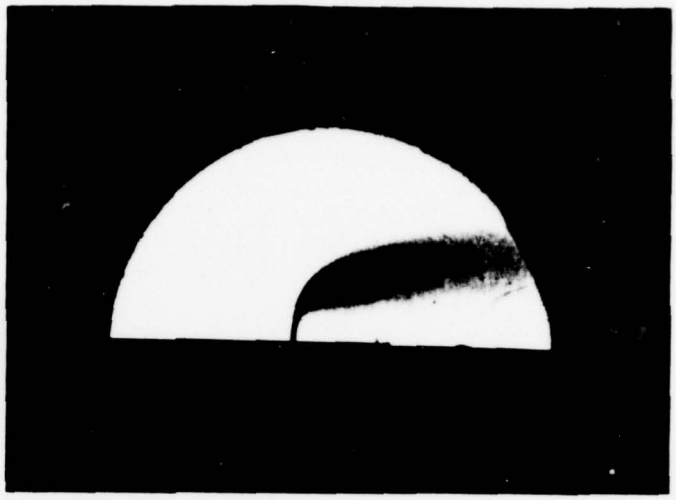

$\bar{q}$=2.07
h=0.0
d=0.5

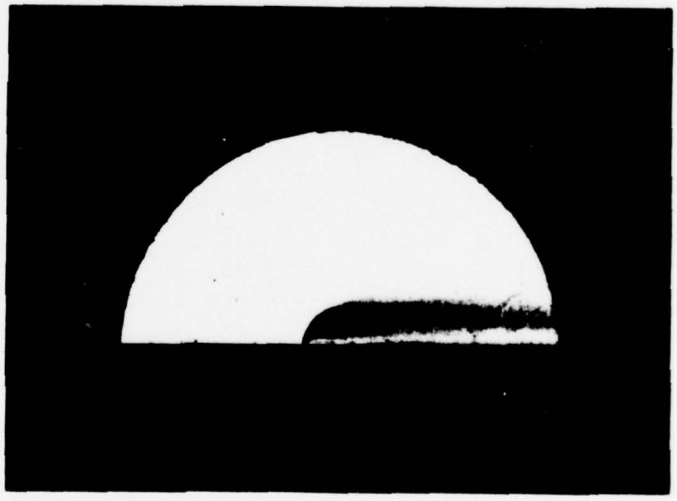

Figure 18. Streak Shadowgraphs of Injection Jet

$\bar{q}$=9.57
h=0.5
d=1.0

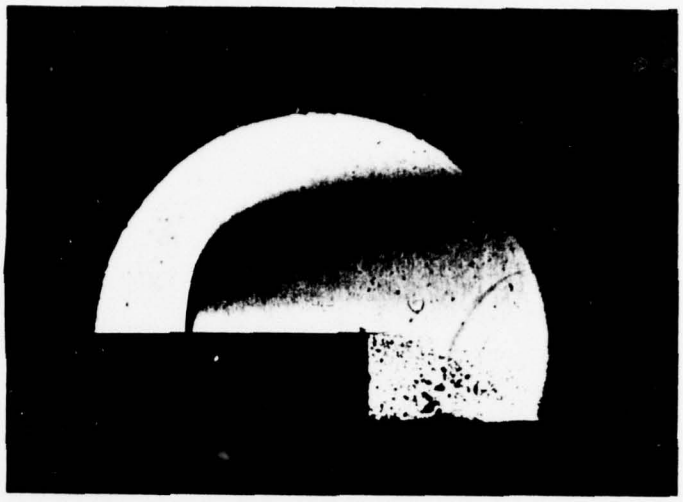

$\bar{q}$=5.12
h=0.5
d=1.0

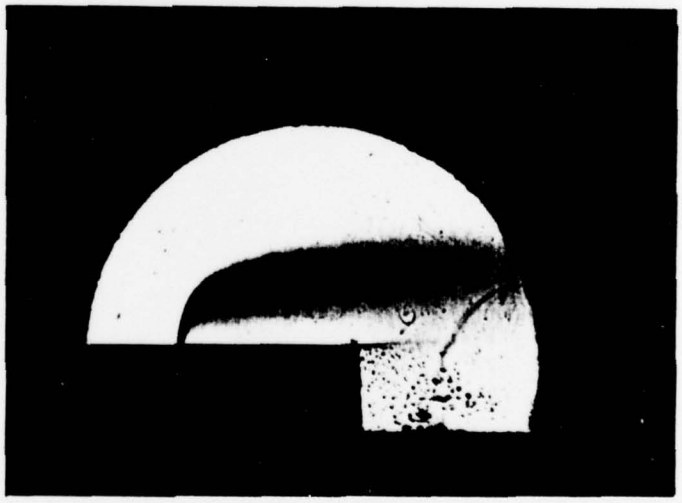

Figure 19. Streak Shadowgraphs of Injection Jet

$\bar{q}$=10.11
h=0.5
d=0.5

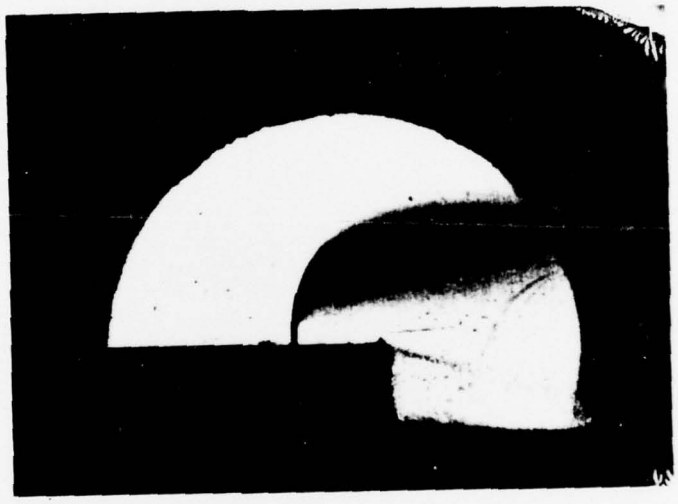

Figure 20. Streak Shadowgraphs of Injection Jet

$\bar{q}$=4.95
h=0.5
d=0.5

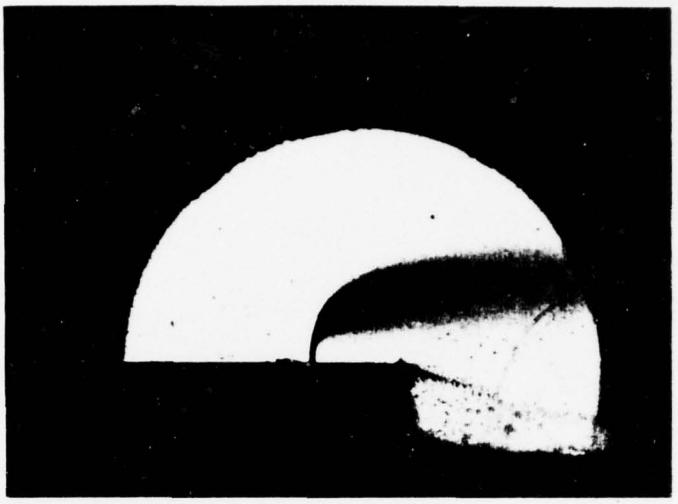

$\bar{q}$=1.95
h=0.5
d=0.5

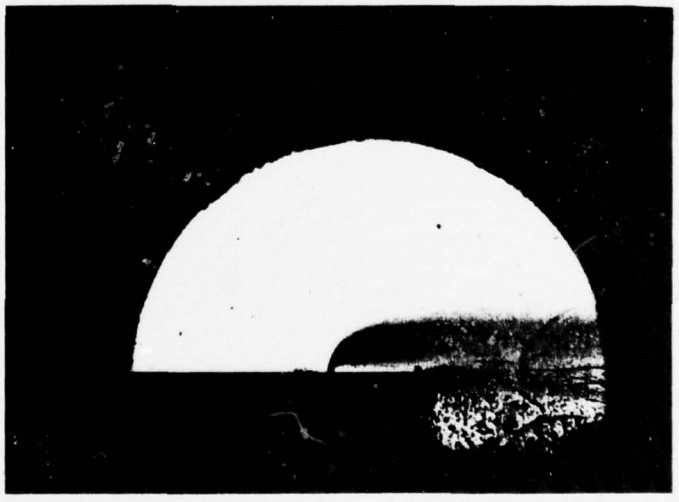

Figure 21. Streak Shadowgraphs of Injection Jet

$\bar{q}$=10.48
h=0.5
d=0.5

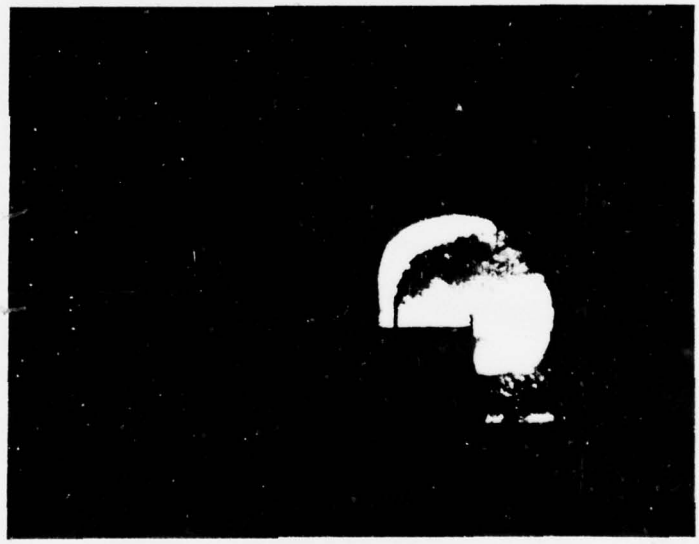

$\bar{q}$=5.15
h=0.5
d=0.5

Figure 22. Spark Shadowgraphs of Injection Jet

$\bar{q}$=1.98
h=0.5
d=0.5

$\bar{q}$=10.21
h=1.0
d=0.5

Figure 23. Spark Shadowgraphs of Injection Jet

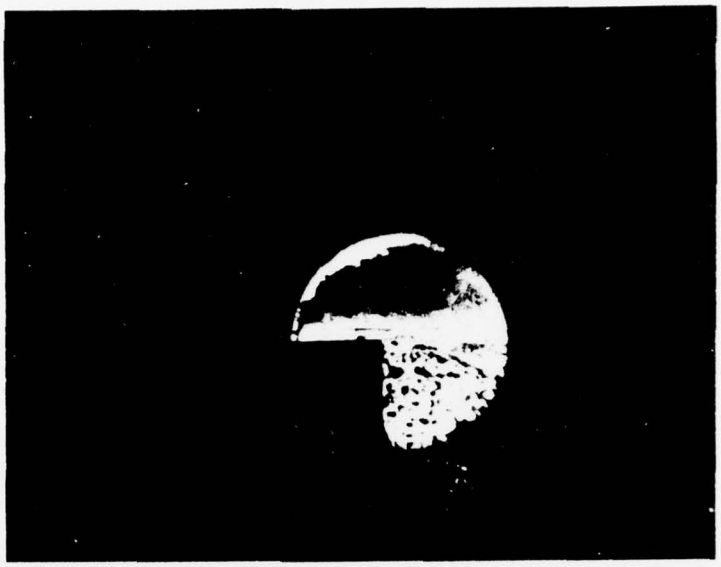

$\bar{q}$=5.06
h=1.0
d=0.5

$\bar{q}$=2.04
h=1.0
d=0.5

Figure 24. Spark Shadowgraphs of Injection Jet

h=1.0
d=1.0

Figure 25. Photograph From Video Tape Showing Water Accumulation

UNCLASSIFIED

SECURITY CLASSIFICATION OF THIS PAGE (When Data Entered)

REPORT DOCUMENTATION PAGE	READ INSTRUCTIONS BEFORE COMPLETING FORM
1. REPORT NUMBER (19) (18) AFOSR-TR- 79-0769 / 2. GOVT ACCESSION NO.	3. RECIPIENT'S CATALOG NUMBER
4. TITLE (and Subtitle) (6) LIQUID FUEL JET INJECTION INTO A SIMULATED SUBSONIC "DUMP" COMBUSTOR	5. TYPE OF REPORT & PERIOD COVERED (9) INTERIM Prepts
	6. PERFORMING ORG. REPORT NUMBER (14) VPI-Aero-093
7. AUTHOR(s) (10) JOHN C. OGG / JOSEPH A. SCHETZ	8. CONTRACT OR GRANT NUMBER(s) (15) AFOSR-78-3485
9. PERFORMING ORGANIZATION NAME AND ADDRESS VIRGINIA POLYTECHNIC INSTITUTE & STATE UNIVERSITY AEROSPACE & OCEAN ENGINEERING DEPARTMENT BLACKSBURG, VA 24061	10. PROGRAM ELEMENT, PROJECT, TASK AREA & WORK UNIT NUMBERS (16) 2308/A2 61102F (17) A2
11. CONTROLLING OFFICE NAME AND ADDRESS AIR FORCE OFFICE OF SCIENTIFIC RESEARCH/NA BLDG 410 BOLLING AIR FORCE BASE, D C 20332	12. REPORT DATE (11) May 1979
	13. NUMBER OF PAGES 57
14. MONITORING AGENCY NAME & ADDRESS (if different from Controlling Office) (12) 64 p.	15. SECURITY CLASS. (of this report) UNCLASSIFIED
	15a. DECLASSIFICATION/DOWNGRADING SCHEDULE

16. DISTRIBUTION STATEMENT (of this Report)

Approved for public release; distribution unlimited.

17. DISTRIBUTION STATEMENT (of the abstract entered in Block 20, if different from Report)

18. SUPPLEMENTARY NOTES

19. KEY WORDS (Continue on reverse side if necessary and identify by block number)
RAMJETS
LIQUID JETS
COMBUSTORS

20. ABSTRACT (Continue on reverse side if necessary and identify by block number)
Basic experimental studies of the injection of liquid fuel into a two dimensional flowfield designed to represent a sudden-expansion "dump" combustor were performed under cold-flow conditions. Test conditions were as follows: 0.6 entrance Mach number, 25 PSIA total pressure, and nominally 75°F stagnation temperature. Two step heights were investigated, 1.0 in. in 0.5 in., corresponding to area ratios of 1.33 and 1.17. The investigation included Pitot and static pressure distributions, spark and streak shadowgraphs, surface flow visualization, direct photographs and videotape recordings. The backlighted streak and spark shadowgraphs were used to

DD FORM 1 JAN 73 1473 406 922 UNCLASSIFIED